

An experimental study on crossing nose damage of railway turnouts in The Netherlands

Markine, VL; Shevtsov, IY

Publication date

2013

Document Version

Accepted author manuscript

Published in

Proceedings of the fourteenth international conference on civil, structural and environmental engineering computing

Citation (APA)

Markine, VL., & Shevtsov, IY. (2013). An experimental study on crossing nose damage of railway turnouts in The Netherlands. In BHV. Topping, & P. Ivanyi (Eds.), *Proceedings of the fourteenth international conference on civil, structural and environmental engineering computing* (pp. 1-11). Civil-Comp Press.

Important note

To cite this publication, please use the final published version (if applicable).
Please check the document version above.

Copyright

Other than for strictly personal use, it is not permitted to download, forward or distribute the text or part of it, without the consent of the author(s) and/or copyright holder(s), unless the work is under an open content license such as Creative Commons.

Takedown policy

Please contact us and provide details if you believe this document breaches copyrights.
We will remove access to the work immediately and investigate your claim.

EXPERIMENTAL STUDY ON CROSSING NOSE DAMAGE OF RAILWAY TURNOUTS IN THE NETHERLANDS

V. L. Markine¹ and I.Y. Shevtsov²

¹Delft University of Technology, Delft, the Netherlands

²ProRail, the Netherlands

Abstract

The dynamic behaviour of turnout crossings is analysed using field measurements. The dynamic responses of a turnout due to passing trains are measured using a mobile device. The main elements of the device are the 3D acceleration sensor (to be installed at the crossing nose), the velocity sensor and the sleeper displacement sensor. The measured dynamic responses of the turnout primarily comprise of the accelerations of the crossing nose and the displacements of a sleeper recorded for the three dimensions. Geometry of the crossing nose of the turnouts has been measured using a laser-based device Calipri.

Based on velocity of the passing trains (which is measured as well) the locations of the maximum accelerations of the crossing nose due to each wheel are derived. These locations indicate the most probable area for initiation of the fatigue defects on the crossing nose.

Using the above-mentioned device a number of turnouts were measured. The dynamic responses were collected and analysed.

From the measured results it was observed that the type of rolling stock and geometry of the crossing nose have strong influence on the location of the impact contact on the crossing nose and finally on its damage.

Based on these results it can be concluded that by proper adjustment of the crossing nose geometry its condition can be controlled and damage to the crossing nose can be reduced.

Keywords: instrumented turnout, wheel/rail contact, crossing nose damage

1 INTRODUCTION

Railway turnouts are important elements of the railway infrastructure, which enables trains to be guided from one track to another at a railway junction as shown in Figure 1.

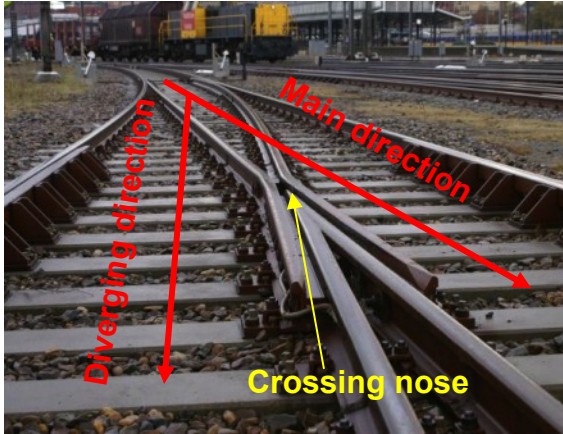


Figure 1 Railway turnout and crossing nose

In this figure it can clearly be seen that at the location of the crossing nose the rail geometry (the inner rail) is discontinuous. Due to such a discontinuity the crossing nose experiences high impact loads from the wheels of passing trains. These forces initiate various types of damage to the crossing nose of the railway turnout (Figure 2). Statistical evidence shows that failures in turnouts cause major operational disturbances in a railway network.

The train and turnout interaction has been analysed both numerically and experimentally in a number of research papers being published recently. Various numerical models for analysis of the dynamic behaviour of turnout can be found in [1]-[6]. Experimental analysis of the turnout behaviour is important as well. It was investigated in a number of papers usually for the purpose of numerical model validation [6]-[8].



Figure 2 RCF damage of crossing nose

In this paper the results of the measurements in the common crossing of turnouts are presented. The measurements were performed within the framework of the project investigating the effects of the vertical elasticity of turnout performance commissioned by ProRail (rail infrastructure provider in the Netherlands) [5]. In the first phase of this project the effects of the elastic elements (such as rail pads, under sleeper pads and ballast mats), vertical rail geometry and sleepers on the dynamic forces in the crossing nose were numerically investigated. The next step in this project was to verify the numerical findings using field measurement.

During the field tests the accelerations of the crossing nose and sleepers due to passing trains on different types of turnouts were measured. Other responses (e.g. fatigue areas on the crossing nose) were derived from the measured acceleration signals. Using the measurements some relationships between the types of the train, train velocities, crossing condition and type of sleepers on one hand and the forces in the crossing nose on the other were established.

The measurement device, the measured and derived data are described in Section 2. The results of the performed field tests are presented and discussed in Section 3. Conclusions are given in Section 5.

2 Measurement devices

The experimental analysis of the dynamic behaviour of turnout crossings was performed here on the basis of the measured geometry and accelerations of the crossing nose. The devices used to collect these data are described below.

2.1 Instrumented crossing

The measurement device ESAH-M for analysis of wheel-rail contact in the crossing area used here consists of the following components:

- The 3D acceleration sensor on a magnet which has to be placed at the side of the crossing nose (Figure 3)
- Two inductive sensors to be installed on the rail on before the crossing nose. Using the distance between the sensors the train velocity can be determined.
- The sleeper displacement sensor (optional) to be place on one of sleepers near the crossing nose
- The main unit, wherein all the signals are received and synchronised.



Figure 3 Acceleration sensor mounted on crossing nose

An example of the raw data i.e. the rail accelerations due to moving train is shown in Figure 4.

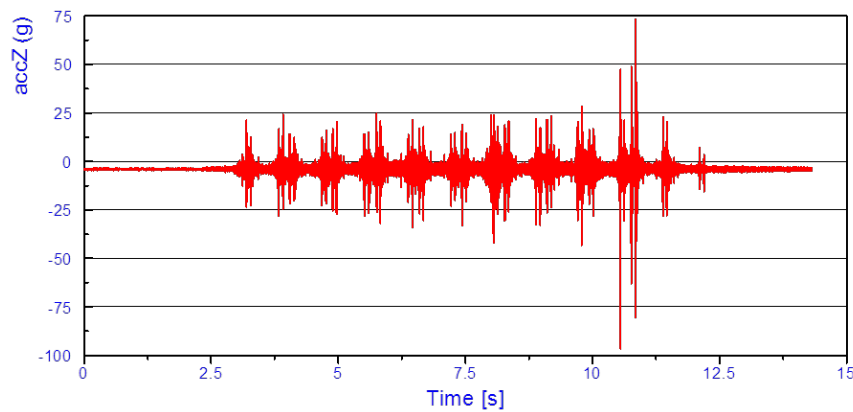


Figure 4 Rail accelerations (crossing nose)

Since the velocity of the passing train and the distance from the velocity sensor to the beginning of the crossing nose are known, it is possible to determine the magnitude and location of the maximum wheel force acting on the crossing nose. The locations of the maximum vertical accelerations of the crossing caused by each wheel, which presumably correspond to the locations of the first impact of the wheel, are presented as the wheel contact distribution histogram (Figure 5). The maximum accelerations are sought within 1m from the beginning of the crossing (point N) based on the wheels velocity and the distance between the velocity sensors and the point N as shown in Figure 5. Based on such a histogram the most probable area for fatigue damage (fatigue area) on the surface of the crossing nose can be determined.

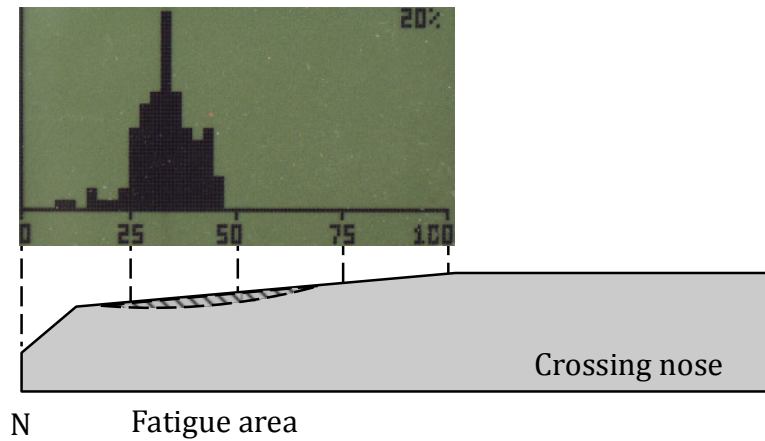


Figure 5 Wheel contact distribution in crossing nose

Other data used here, which is derived from the measured accelerations, is the maximum acceleration of the crossing nose caused by each wheel of the passing train. An example of such a plot is shown in Figure 6. In this figure the maximum vertical, lateral and total accelerations of the rail per wheel are shown. Based on this data the wheel forces can be estimated and the quality of each wheel can be assessed.

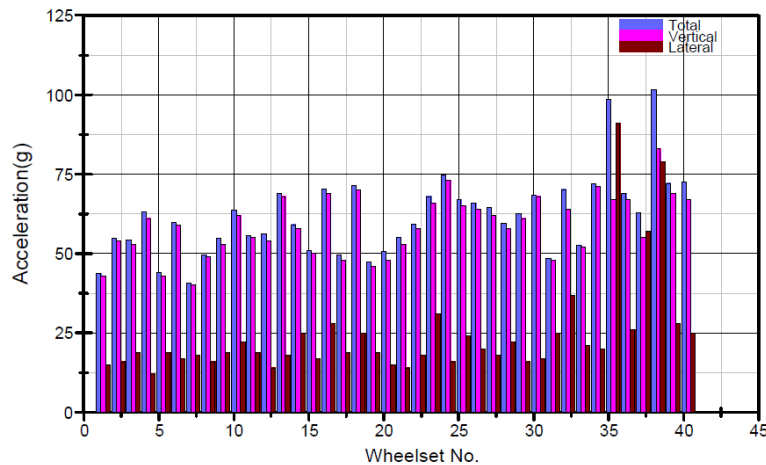


Figure 6 Maximum rail (crossing nose) accelerations due to wheels of passing train

2.2 Crossing nose geometry

Crossing nose geometry was measured using the laser-based devices called Calipri. The device can measure cross-sectional geometry of railway wheels and rails including turnouts. The cross-sectional geometry of the rail is measured in a number of the locations along the turnout as shown in Figure 7.

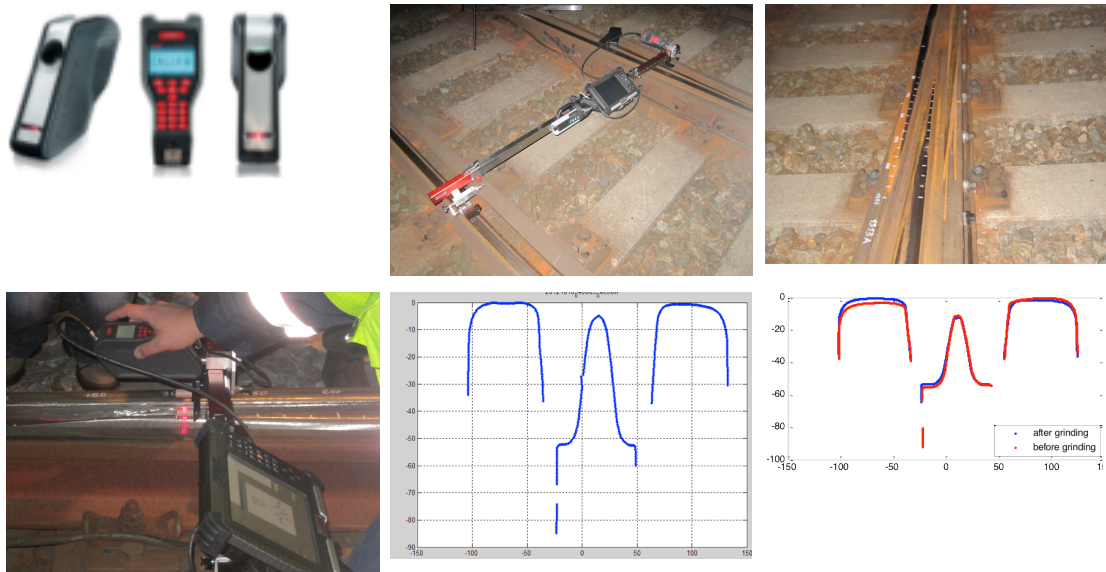


Figure 7 Rail geometry measurement device Calipri

3 Measurements

The measurements using the above-mentioned devices were performed on a numbers of turnouts in different locations in the Netherlands. Some results were presented earlier in [11]. Here the measurements from turnouts with the angle 1:15 on concrete sleepers from two locations are presented. The trains were passing with their operational velocities. To assess the performance of the measured turnouts (and the wheel quality of the passing trains) the following responses were obtained:

- Maximum vertical and lateral accelerations of the crossing due to passing wheels (contact forces)
- Wheel contact distribution (fatigue area) along the crossing nose
- Rail cross-sectional geometry along the crossing nose.

Apart from the measured data from the instrumented turnouts visual images of the rail surfaces were taken as well. The measurement results are presented and discussed below.

4 Results and discussion

The measured results were collected and analysed. Using these measurements the conclusions presented in [11] have further been confirmed, namely that the rail geometry and the rolling stock have significant effect on the wheel-rail contact forces acting in the turnout crossing. The results and conclusions are presented below.

4.1 Rolling stock

The measurements with the ESAH-M device have been performed on a 1:15 turnout while various trains were passing it. The passing trains were intercity (VIRM and ICM) and local (Sprinter and ICMat) ones as shown in Figure 8.

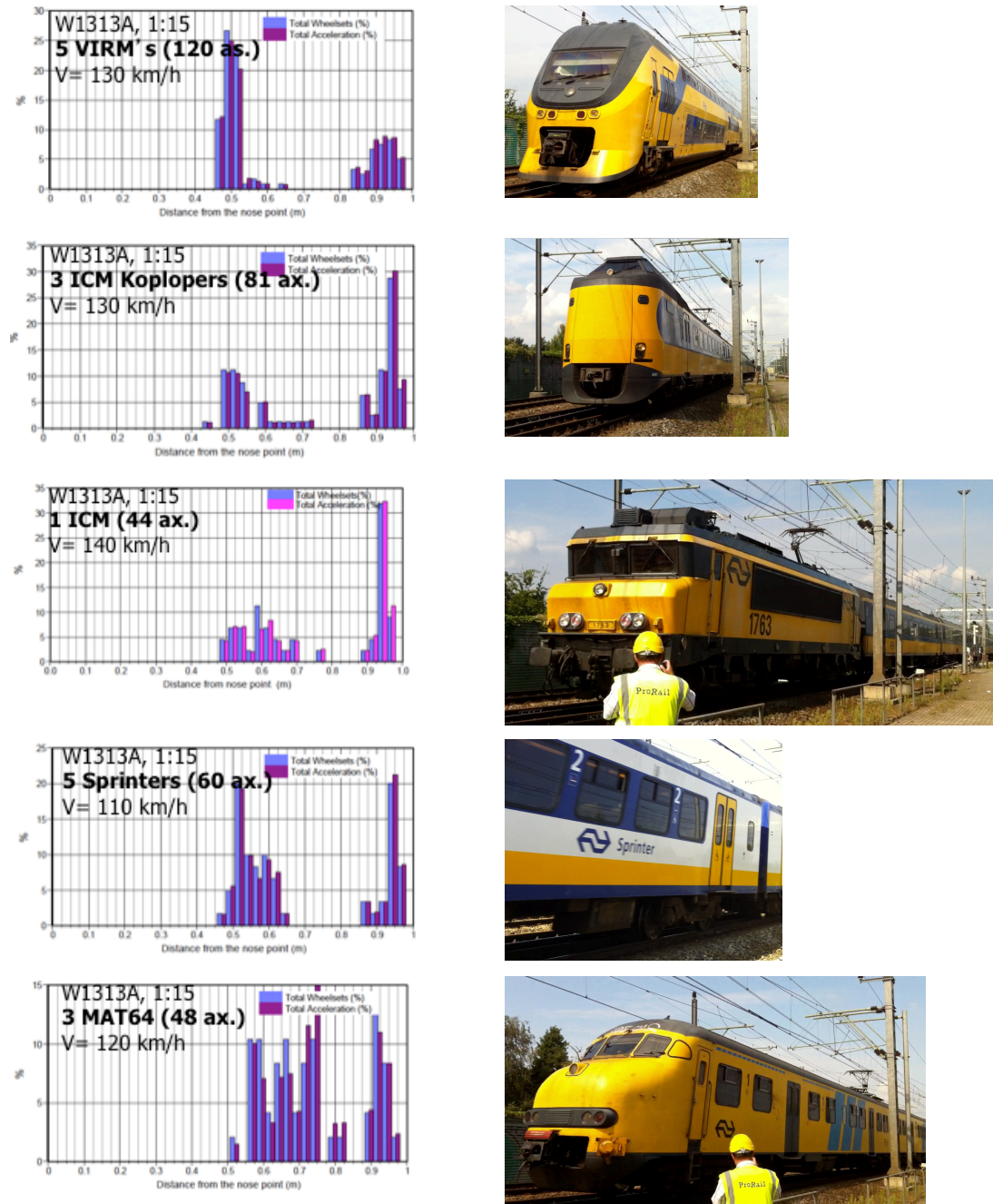


Figure 8 Distribution of maximum wheel force along crossing nose due to different type of trains

From this figure two rail fatigue locations can clearly be seen, namely around 0.5m-0.6m and 0.9m from the beginning of the crossing nose. Also, it can be seen that different type of rolling stock has different impact on the crossing nose. In particular, the wheel impact forces of the intercity trains and sprinter are concentrated around these two locations while the forces of the local MAT64 trains are spread on the area between 0.55m-0.95m. This can be explained by the fact that MAT64 rolling stock is quite old. It can also be seen that the VIRM trains have highly concentrated impact forces around 0.5m, which in case of mono (VIRM) traffic can result in fast degradation of the crossing nose.

4.2 Rail geometry

The measurement results presented in [11] have shown that the vertical geometry of the crossing nose had strong influence on the impact point distribution. In this Section the effect of the 3D rail geometry on distribution of the impact wheel forces is discussed. The considered turnout has the crossing angle of 1:15. The crossing nose geometry and wheel forces of a turnout have been measured before and after grinding of the crossing nose. The grinding of the crossing nose was a part of damage repair procedure consisting of removal of the damaged material, adding (welding) additional one and re-profiling (grinding) of the crossing nose. Some stages of the crossing nose repair procedure are shown in Figure 9.

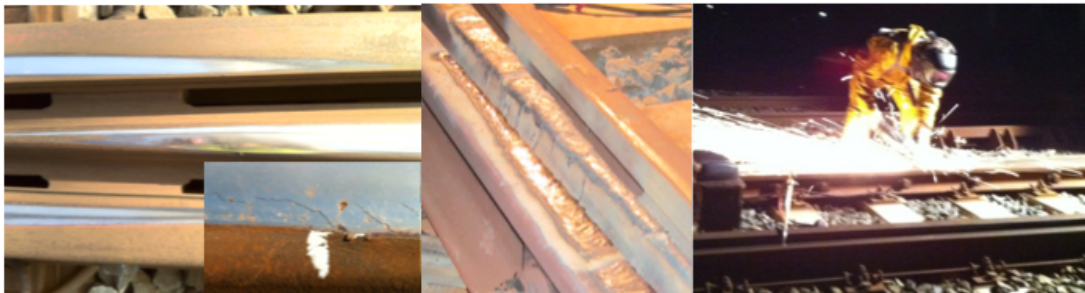


Figure 9 Crossing nose repair procedure

It should be noted that the crossing nose geometry after grinding to a large extent depends on the skills and experience of the grinder. Moreover, the original (manufacturer) geometry is not always restored. This is the case with the crossing nose considered here. The grinder has made some adjustments in the wing rail and crossing nose geometry based on his observations of the rail damage.

The adjustment in the rail geometry has resulted in the number of changes in the dynamic responses of the crossing nose, which are discussed below. It should be noted that majority of the passing trains on this turnout were of the same type, namely the intercity trains VIRM (Figure 8) and the passing speed was around 135 km/h. The number of the passing trains measured before and after the grinding was 20 (736 axles) and 18 (496 axles) respectively.

The distribution of the maximum wheel forces along the crossing nose before and after grinding is shown in Figure 10. From this figure it can be seen that the force

distribution after the grinding has become wider. Most of the wheel impacts on the crossing nose before the grinding were very much concentrated in the range 0.5m-0.6m (which finally resulted in damage in this area – 0.55m), while after the grinding only 30% of the impact forces were in this range. The widening of the fatigue area can have a positive effect on reduction of crossing nose damage.

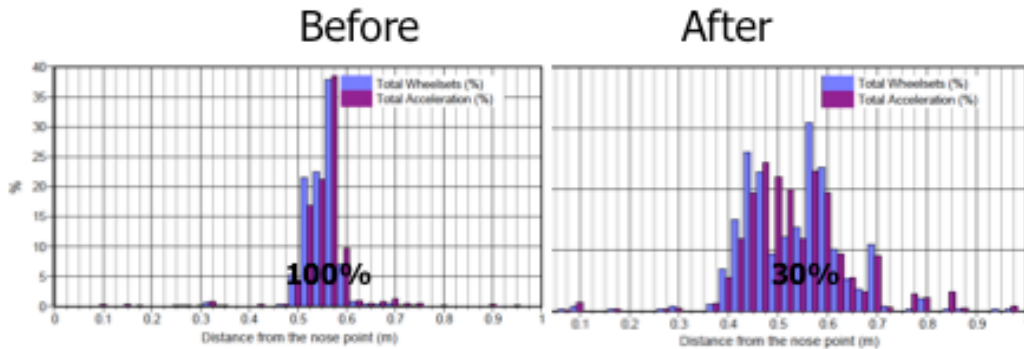


Figure 10 Wheel forces distribution before and after grinding

The adjustments in the crossing geometry has also resulted in the reduction of the magnitude of the impact forces as it can be seen from Figure 11. In this figure the wheel force registrations of two train passages are shown. The average wheel force was reduced by the factor 1.7. The reduction of the impact force magnitude has also a positive effect on reduction of damage to the crossing nose.

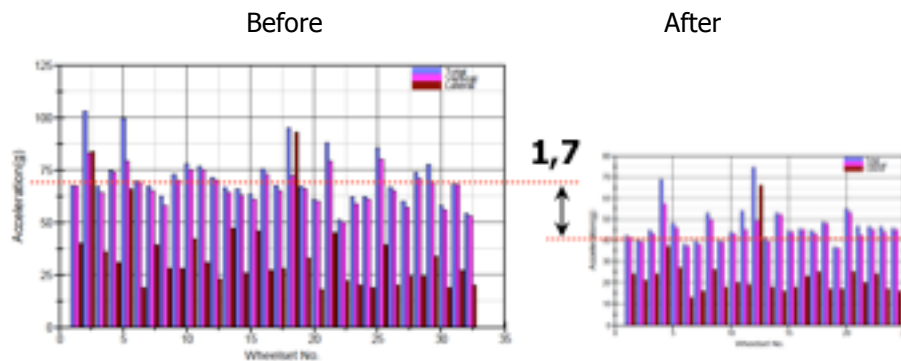


Figure 11 Reduction of magnitude of wheel forces due to geometry adjustments

From the measured results it was also observed that the magnitude of some incidental high forces was extremely increased. An example of such forces is shown in Figure 12. The ratio average/max force in this figure before and after the grinding is respectively 75/200 and 50/500. The increase of the magnitude of the incidental forces can be explained by the nature of these forces. Before the grinding such forces were mostly due to bad wheels, while after the grinding these forces are due to imperfections of the new geometry. The high forces result in plastic deformations in the rail due to which the rail imperfections will disappear and the incidental forces then will be of the same order as before the grinding.

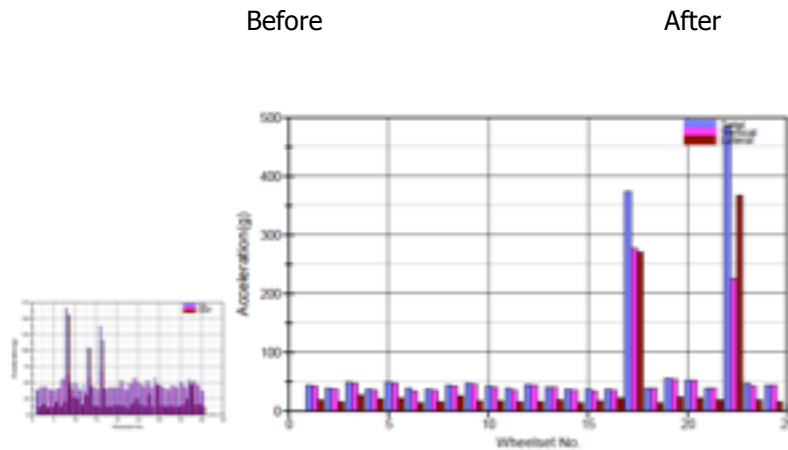


Figure 12 Incidental high forces before and after grinding

These results have shown that maintaining the crossing nose geometry is important for controlling the wheel-rail contact forces in turnout. Also these results have confirmed the numerical results obtained earlier in this project [10].

5 Conclusions

The accelerations of the crossing nose of turnouts with the angle of 1:15 due to various trains were measured. The vertical geometry in the crossing nose was obtained as well by using a laser-based device. Based on these measurements the maximum wheel forces acting on the crossing nose and impact distribution plots indicating the fatigue areas in the crossing nose for each passing wheel were obtained.

From the measured results it was observed that the type of rolling stock and geometry of the crossing nose have strong influence on the location of the impact contact on the crossing nose and finally on its damage.

Based on these results it can be concluded that by proper adjustment of the crossing nose geometry its condition can be controlled and damage to the crossing nose can be reduced.

References

- [1] Kassa, E., Andersson, C. and Nielsen, J.C.O. (2006) Simulation of dynamic interaction between train and railway turnout, Vehicle System Dynamics,

- March 2006, Vol. 44, No.3, pp. 247-258.
- [2] Wiest, M., Daves, W., Fischer, F.D. and Ossberger, H. (2008) Deformation and damage of a crossing nose due to wheels passages. *Wear*, Vol. 265, pp. 1431-1438.
 - [3] Andersson, C. and Dahlberg, T. (2000) Load impacts at railway turnout crossing, *Vehicle System Dynamics*, 2000, vol. 33, SUPPL, pp. 131 – 142.
 - [4] Alfi, S. and Bruni, S. (2009) Mathematical modelling of train-turnout interaction, *Vehicle System Dynamics*, 47:5, 551- 574.
 - [5] Markine, V.L., Steenbergen, M.J.M.M. and Shevtsov, I.Y. (2011) Combatting RCF on switch points by tuning elastic track properties, *Wear* 271 (2011), pp. 158-167. doi:10.1016/j.wear.2010.10.031
 - [6] Wan, C., Markine, V.L. and Shevtsov, I.Y. (2012) Simulation of Train-Turnout Interaction and Validation using Field Measurements. In *Proceedings of the First International Conference on Railway Technology: Research, Development and Maintenance*, J. Pombo, (Editor), Civil-Comp Press, Stirlingshire, United Kingdom, paper 136, 2012. doi:10.4203/ccp.98.136
 - [7] Kassa, Elias and Nielsen, Jens C. O.(2008) 'Dynamic interaction between train and railway turnout: full-scale field test and validation of simulation models', *Vehicle System Dynamics*, 46: 1, 521 — 534. DOI: 10.1080/00423110801993144
 - [8] Cornish, A., Kassa, E. and R. Smith, R. (2012) Field Experimental Studies of Railway Switches and Crossings. In *Proceedings of the First International Conference on Railway Technology: Research, Development and Maintenance*, J. Pombo, (Editor), Civil-Comp Press, Stirlingshire, United Kingdom, paper 137, 2012. doi:10.4203/ccp.98.137
 - [9] Markine, V.L. (2012) Dynamic Response Measurements of Common Crossings. Research commissioned by ProRail. TU Delft report 7-12-234-03. ISSN 0169-9288
 - [10] Markine, V.L. and Steenbergen, M.J.M.M. (2009) Elasticiteit Wissels Op Betonnen Dwarsliggers. Rapportage fase 02, 04 van het onderzoek in opdracht ARCADIS/ProRail. TU Delft report 7-09-234-01. ISSN 0169-9288 (In Dutch)
 - [11] Markine, V.L. and Shevtsov, I.Y. (2012) Experimental Analysis of the Dynamic Behaviour of Railway Turnouts. In Topping, B.H.V., ed. *The Eleventh International Conference on Computational Structures Technology* (Civil-Comp Press, Dubrovnik, Croatia, 2012).